Received: 23 November 2022 | Revised: 19 January 2023 | Accepted: 30 January 2023

DOI: 10.1002/appl.202200113

RESEARCH ARTICLE

Applied Research

MOKE and MFM on magnetically coated nanofiber mats: Transferring well-known methods to uncommon samples

Oliver Brocks[1] | Adam Stasiak[2] | Jan Biedinger[3] | Martin Wortmann[3] | Tomasz Blachowicz[2] | Reinhard Kaschuba[1] | Andrea Ehrmann[1]

[1]Faculty of Engineering and Mathematics, Bielefeld University of Applied Sciences, Bielefeld, Germany

[2]Institute of Physics - Center for Science and Education, Silesian University of Technology, Gliwice, Poland

[3]Faculty of Physics, Bielefeld University, Bielefeld, Germany

Correspondence
Andrea Ehrmann, Faculty of Engineering and Mathematics, Bielefeld University of Applied Sciences, Bielefeld, Germany.
Email: andrea.ehrmann@fh-bielefeld.de

Abstract

The hysteresis loops of magnetic samples can be measured by the magneto-optical Kerr effect (MOKE), while magnetic force microscopy (MFM) is used to depict domain walls or spatially resolved magnetization orientation in magnetic nanostructures or thin films. Both methods are commonly applied on thin films with a perfectly flat surface or on nanostructures. Here, we report MOKE and MFM measurements on a new class of magnetic materials, namely electrospun mats of randomly oriented nanofibers which influence the 30 nm Co coating layer, proving especially the MOKE method utilizable for rough surfaces. Possible interpretations of these first MOKE measurements on highly randomly structured magnetic layers are given.

KEYWORDS

diode bridge, electrospinning, magnetic force microscopy, magnetic nanofiber mats, magneto-optical Kerr effect, magnetron sputtering

INTRODUCTION

Magnetic nanofibers can be produced by electrospinning, for example, by embedding magnetic nanoparticles into the spinning solution or by coating them in a postprocessing step [1–3]. Such magnetic nanofibers can be applied, for example, for electromagnetic shielding, sensors, spintronics devices, or neuromorphic computing [4–6].

Examinations of magnetic nanofibers mats are usually performed by SQUID [7], AGM [8], VSM [9], or other magnetometers, which average over the full sample and thus impede investigating position-dependent differences in the magnetic properties. Mapping magnetic properties of thin film samples can be done by different techniques. The magneto-optical Kerr effect (MOKE) enables resolutions of some 10 µm in a normal setup, measuring the rotation of the linear polarization of a laser beam reflected by the sample. A MOKE microscope allows for investigating the in-plane magnetization on typical length scales of optical microscopes [10] and is scarcely reported for single nanofibers [11]. Much higher resolutions are enabled by magnetic force microscopy (MFM), an extension of atomic force microscopy (AFM), at the cost of increased measurement time [12].

MOKE measurements can be performed with the high magnetic resolution, if a diode bridge is used [13], usually in combination with a chopper triggering a lock-in amplifier. Nevertheless, reports of MOKE measurements on irregular uneven surfaces are scarcely reported in the literature, giving evidence for the possibility to measure MOKE in principle also on coatings with micrometer roughness or uneven bulk materials, as long as the reflection of the laser beam impinging on the sample is oriented in a narrow-angle around the specular reflection [14, 15]. It should be mentioned that measuring MOKE on regular uneven surfaces,

such as nanostructure arrays, is unproblematic [16, 17]; the different diffraction orders, available under different reflection angles, even give rise to more information about the magnetic properties of the sample under investigation than the common zeroth-order MOKE signal [18].

MFM measurements, on the other hand, have the problem that with increasing surface roughness in fiber-based materials, distinguishing between magnetic and topographic features becomes more and more complicated, while at the same time, a high surface roughness in the range of several hundred nanometers necessitates modification of the measurement parameters in such a way that the lateral resolution is significantly reduced [19]. Thus, only a few attempts to measure MFM on single nanofibers are reported in the literature [20–24], with a first preliminary study from our group indicating that MFM on nanofiber mats can generally give a magnetic signal [25].

Here, we report on the characterization of a magnetic nanofiber mat with random fiber orientation and magnetic coating by MOKE and MFM. Both measurement techniques are shown to work for irregular electrospun nanofiber mats for the first time and will enable easier and faster examination of such irregular magnetic structures in the future.

MATERIALS AND METHODS

Nanofiber mats were prepared with the wire-based electrospinning machine "Nanospider Lab" (Elmarco Ltd.). The spinning parameters were: voltage 80 kV, nozzle diameter 0.9 mm, carriage speed 100 mm/s, the distance between the bottom electrode and substrate 240 mm, the distance between the ground electrode and substrate 50 mm, the temperature in the spinning chamber 23–24°C, and relative humidity 32–33%. Spinning solutions were prepared by dissolving 16 wt% polyacrylonitrile (PAN) in dimethyl sulfoxide (DMSO) (min. 99.9%, purchased from S3 Chemicals) ("PAN nanofiber mat") or by dissolving 15 wt% PAN and 5 wt% ZnO (nanopowder <100 nm particle size; Sigma-Aldrich) in DMSO ("PAN/ZnO nanofiber mat"). Images of the nanofiber topography and further information can be found elsewhere [26]; nanofiber diameters are in the range of 140 nm ± 40 nm (PAN) or 450 nm ± 120 nm (PAN/ZnO), respectively. These different nanofiber diameter distributions were chosen to investigate whether the diffraction of the reflected laser beam on surfaces with different length scales of alternating fibers and pores between them will result in different signals. Besides, PAN films were prepared using a doctor's blade with a wet film thickness of 30 µm.

Parts of these three samples were mounted on a Si(100) wafer and, together with the residual wafer, coated with 30.5 nm Co (layer thickness measured by X-ray reflectivity). No additional capping layer was applied so that the Co layer was naturally oxidized. The Co thin film was prepared via DC magnetron sputtering at room temperature in an ultrahigh vacuum sputter deposition system (BesTec GmbH) with a base pressure lower than 10^{-8} mbar. The sputtering power from the elemental 3″ Co target (99.95% purity; HMW Hanauer GmbH & Co. KG) was set to 150 W. A gas flow of 10 sccm high-purity Ar (99.99999%; Linde GmbH) was adjusted, resulting in a working pressure of 2.8×10^{-3} mbar during sputtering. The deposition rate was determined to be 0.083 nm/s. The roughness R_a of both the Co-coated PAN film and the Co-coated Si wafer is 2–4 nm, depending on the sample position. For the Co-coated nanofiber mats, the roughness R_a can even be below 1 nm, if measurements are performed parallel to the fiber axis since electrospun nanofibers without large amounts of inorganic blends are automatically highly even due to the production process.

AFM and MFM were measured by a FlexAFM Axiom (Nanosurf) in tapping mode (setpoint 60%, P-gain 550, I-gain 1000, D-gain 0, vibration amplitude 4 V), using a Multi 75M-G magnetic cantilever. The tip was magnetized perpendicular to the sample surface; the samples were investigated after being set to their coercive fields (in the case of Co-coated PAN film and nanofiber mats), using the MOKE magnetic field, or after being magnetized out-of-plane (in the case of the wafer coated with Co), respectively. MFM measurements were taken in dual-pass mode at a lift height of 50 nm, that is, the MFM image is taken by following the AFM contour with a constant 50 nm distance between tip and sample. Smaller lift heights will result in too much topographic information remaining visible, while larger lift heights will smear out the magnetic information so that a correlation with the topographic information is impeded. AFM and MFM images were postprocessed by Gwyddion 2.58 software.

MOKE measurements were performed by a custom-made optical setup with a diode bridge [13] without a lock-in amplifier, using an in-plane magnetic field. Kerr loops were taken using a horizontal plane of incidence of the p-polarized laser light (633 nm, max. 4 mW). A more detailed description of MOKE measurements with a diode bridge is given in Tillmanns et al. [13]. All measurements were taken at room temperature (~24–25°C) and averaged over eight cycles.

RESULTS

Figure 1 depicts the results of MOKE measurements on the Co-coated Si wafer and on the Co-coated PAN film. The Kerr rotation is given as the relative change of the diode bridge signal, which is the relative difference between the signals on both diodes A and B, that is $(A - B)/(A + B)$. Both signals are clearly visible; the hysteresis loop measured on the PAN film does not show more noise than the one measured on the wafer although the film has a significantly higher waviness, but not a high roughness, that is, it looks shiny like a strongly distorted mirror surface. It should be mentioned that these hysteresis loops can be measured approximately identically on different positions of the samples, besides some rougher positions on the Co-coated PAN film where the manual coating process has led to undesired disturbances of the homogenous film morphology.

The differences in the coercive fields may be attributed to a slightly increased surface roughness of the PAN film as compared to the wafer, as was reported before for Co thin films [27]. This may be interesting for further examinations of thin films on such uneven substrates, since the exchange bias—a unidirectional anisotropy occurring in coupled ferromagnetic/antiferromagnetic systems, such as the here examined Co/CoO at lower temperatures [28]—may also be increased with increasing roughness [29].

Figure 2 shows hysteresis loops measured on the Co-coated nanofiber mats on two arbitrarily chosen positions per sample (Pos. 1 and Pos. 2); approximately 10 positions per sample were examined and delivered very similar signals. Unexpectedly, the noise is not much higher than in the previous measurements, although the absolute signal on each diode was reduced by two orders of magnitude as compared to MOKE measurements on flat surfaces. This shows that although approximately 99% of the laser light reflected from the sample surface does not reach the diodes, measurements are still possible. Opposite to common diode bridge measurements, the measurement results are highly susceptible to stray light or vibrations due to the low signal intensity. As expected, the signals measured on the Co-coated nanofiber mats are position-dependent due to the curvature of the magnetic coating varying with the position on the sample. On the other hand, the magnetic coating on the PAN/ZnO nanofiber mat, consisting of significantly thicker fibers than the pure PAN nanofiber mat, does not give clearly different signals than the coating on the PAN nanofiber mat, indicating that diffraction effects influence the measurements in both cases.

The unusual shapes of the hysteresis loops, including clearly visible asymmetries, have to be discussed. Tests with s-polarized light showed similar shapes, while measurements with 45° polarized light did not reveal transverse signals (cf. [13] for a variation from s to p polarized light, showing longitudinal hysteresis loops for s and p and transverse signals at 45° polarization), underlining that the measured signals must be magnetic ones. However, a polar component could not be ruled out with the recent setup. At room temperatures, strong exchange bias effects can also be excluded.

A more reliable interpretation, however, is given by diffraction on the nanofibers with diameters of a few hundred nanometers, that is, by measuring diffractive effects on the samples. Usually, diffractive MOKE (D-MOKE) is measured on periodically distributed nanoobjects on a surface, that is, nanostructure arrays, bit-patterned media, and so forth [30]. The results show strong similarity to sets of D-MOKE signals of the zeroth to the fourth order as given in figs. 4.5–4.21 of Ref. [30]. Nevertheless, it must be mentioned that the situation here is different—diffraction from a chaotic surface does not enable detecting different diffraction orders with corresponding information inside. Instead, a highly chaotic superposition of reflected beams will contribute to the measured signals. Future simulations of diffraction on different nanofiber mat surfaces are necessary to better understand the effect of constructive and destructive interference in the measured MOKE signals.

A comparison of different sampling regions, as seen in Figure 2, illustrates the high morphological and thus magnetic variance of the Co coating, which is due to the random orientation of the nanofibers.

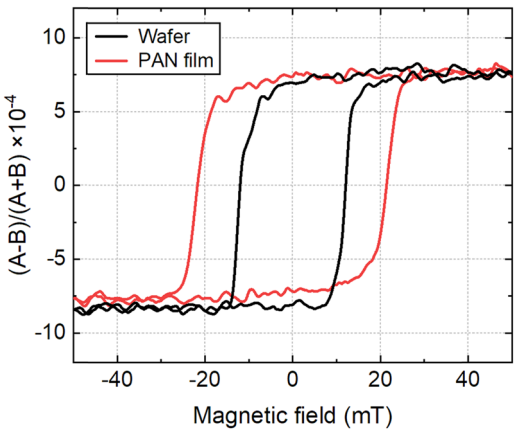

FIGURE 1 Kerr rotation measured on Co-coated Si wafer and polyacrylonitrile (PAN) film.

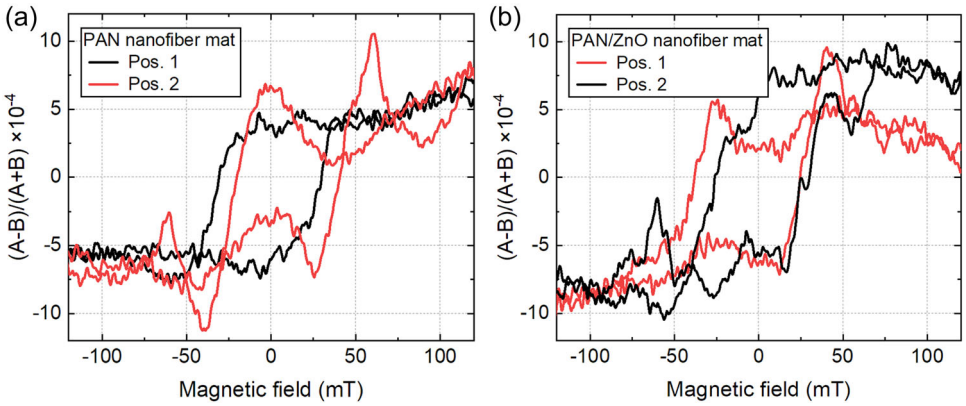

FIGURE 2 Kerr rotation measured on different positions (Pos. 1 and Pos. 2) of Co-coated (a) PAN nanofiber mats; (b) PAN/ZnO nanofiber mats. PAN, polyacrylonitrile.

As discussed in [30], the D-MOKE signals depend on the nanofiber diameters, distances, and curvatures. Future studies will thus explore ways to tailor magnetic properties based on fiber morphology.

In spite of the similarity of these signals with typical D-MOKE signals, as shown in [18] or [30], it must be mentioned that the asymmetries visible here are unexpected. Additional measurements showed that the signals measured were strongly dependent on the position of the impinging laser beam on the sample, but nearly independent from the position of the lens and pinhole collecting the reflected beam. Besides, as there are no regular structures in electrospun nanofiber mats, there are no clear diffraction spots defining zeroth and higher order D-MOKE signals. The interpretation of the measured signals as potential D-MOKE signals can thus be used as a base for further evaluation but needs more MOKE measurements combined with other established methods, such as SQUID, ideally not only of longitudinal hysteresis loops but also of transverse and polar signals.

Finally, AFM and MFM images were taken on these samples. Generally, differentiating between morphology and the magnetic signal is not easy for samples with such large height differences between neighboring structures, as they occur in nanofiber mats, that is, height ranges of several hundred nanometers or more, which are much larger than typical lift heights during the second scan of a dual-scan MFM measurement. Figure 3 shows different AFM and MFM measurements on a cobalt-coated nanofiber mat with an uneven surface in addition to a magnetic signal.

First, the pure morphology of a cobalt-coated nanofiber mat is depicted in Figure 3, measured by the *z*-axis signal of the common AFM measurement. A much sharper signal is visible in the AFM phase (Figure 3b) and AFM amplitude (Figure 3c), respectively. While the AFM amplitude can be used to increase the visibility of edges, the AFM phase additionally shows material differences in a qualitative way [19]. Comparing Figure 3b,c thus suggests that the dark lines in Figure 3b correspond to material differences, for example, missing coating in the three dark lines perpendicular to the fiber axis.

Next, Figure 3d–f shows the same images in MFM mode, that is, at a lift height of 50 nm. As expected, no signal is visible on the *z*-axis (Figure 3d) since short-range interactions with the surface morphology are not possible at this height. Depending on the Gwyddion program settings, the image appears completely black or completely bright yellow, since there are no height differences detectable at the mentioned lift height, as visible in the false color ruler showing 0 m at both ends. While the MFM amplitude (Figure 3f) mainly shows the nearly horizontal groove between the upper and the lower fiber visible in this image, the MFM phase (Figure 3e) clearly differs from Figure 3b. Both lower dark lines are nearly vanished, while the upper one is prominently visible, showing a slightly different shape than in Figure 3b. Obviously, the MFM phase shows out-of-plane magnetization (due to the magnetization of the tip perpendicular to the sample surface, only out-of-plane stray fields of the sample can be detected [19]), that is, a domain wall or our-of-plane stray fields along the dark area. This area is less symmetric than domain walls found in perfectly symmetrical nanostructures [31], as can be expected due to the irregular nature of the nanofiber mat.

Figure 4 depicts more exemplary images of the topography and the magnetic signal of the Co-coated wafer, PAN film, and PAN/ZnO nanofiber mat. The sample depicted in Figure 3 is shown here again (Figure 4c,g) to enable easier comparison with the other samples. On the Si wafer, no domain walls or out-of-plane stray fields could be observed when the sample was set to its coercive field on various dimensions. Instead, Figure 4e depicts an MFM image after out-of-plane magnetization of the sample, resulting in some dark areas,

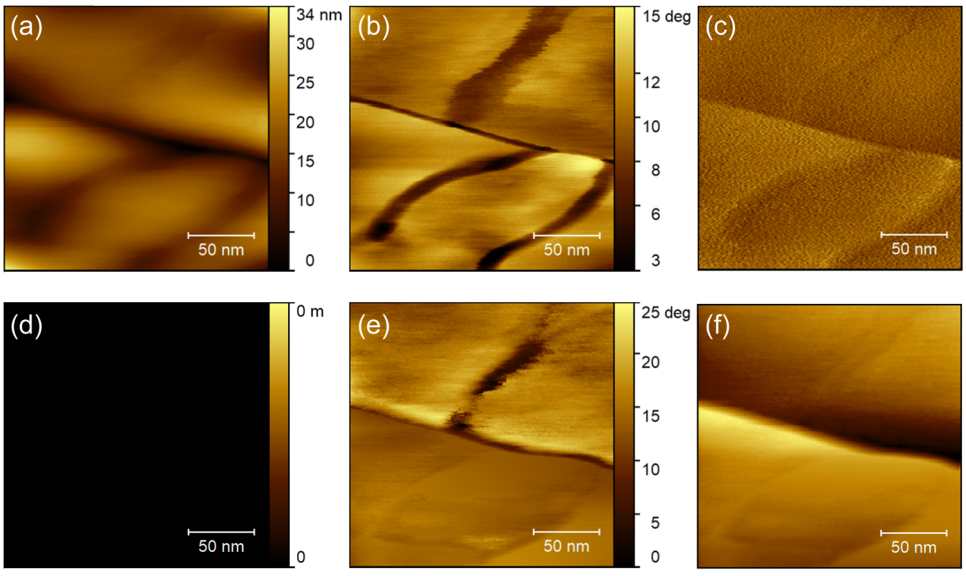

FIGURE 3 AFM/MFM images taken on a PAN/ZnO nanofiber mat: (a) AFM *z*-axis; (b) AFM phase; (c) AFM amplitude; (d) MFM (second scan) *z*-axis; (e) MFM (second scan) phase; (f) MFM (second scan) amplitude. AFM, atomic force microscopy; MFM, magnetic force microscopy; PAN, polyacrylonitrile.

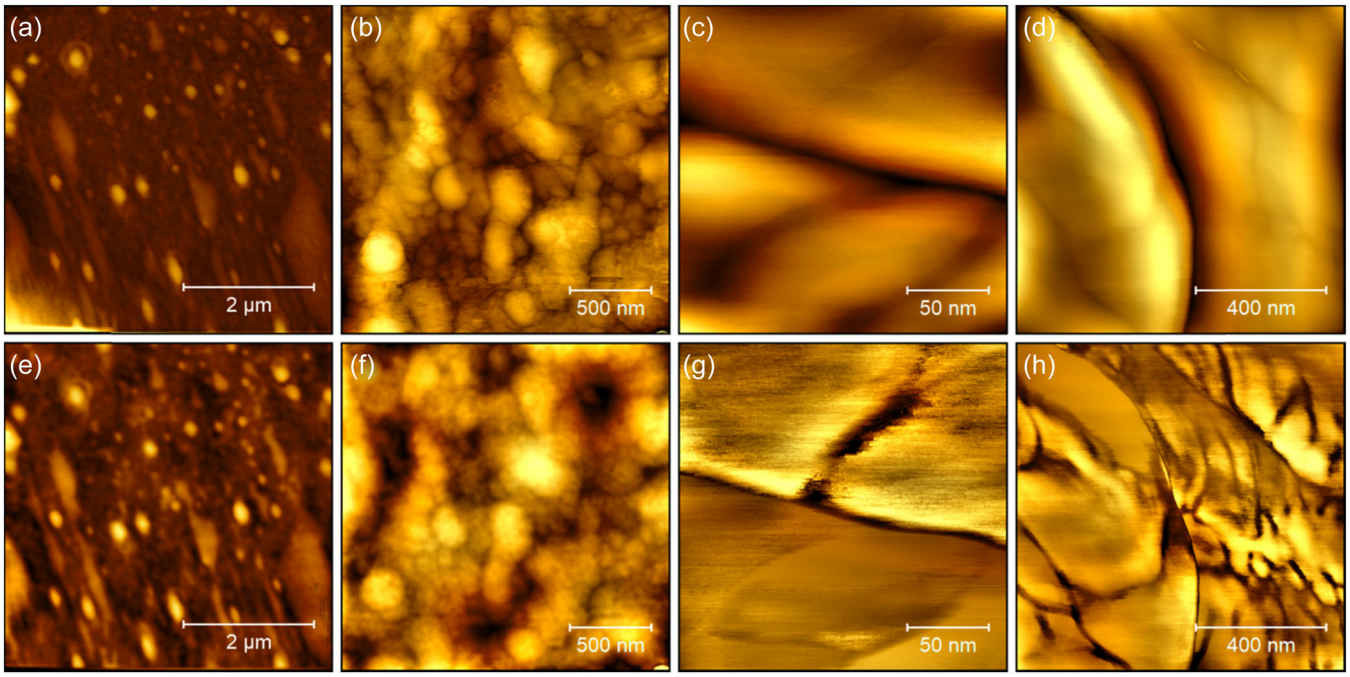

FIGURE 4 (a–d) AFM *z*-axis and (e–h) MFM images (lift height 50 nm) of Co-sputtered (a, e) wafer, (b, f) PAN film, (c, d, g, h) PAN/ZnO nanofiber mat. The magnifications differ. Amplitude ranges for the AFM images are (a) 53 nm, (b) 69 nm, (c) 34 nm, and (d) 131 nm, respectively. Phase ranges of the MFM images are (e) 3.7°, (f) 4.1°, (g) 25°, and (h) 46°, respectively. AFM, atomic force microscopy; MFM, magnetic force microscopy; PAN, polyacrylonitrile.

indicating magnetization orientation slightly opposite to the tip orientation. In the Co layer on the PAN film, the AFM image (Figure 4b) shows a granular topography, while the MFM image (Figure 4f) reveals distinct brighter and darker areas, with the magnetization pointing parallel and antiparallel to the tip, respectively. The occurrence of clusters in sputter coatings on polymer surfaces is a well-known phenomenon [32] and can serve as an explanation for the different coercive fields found on the waver and on the polymer film (Figure 1).

AFM measurements on nanofiber mats are generally challenging due to the large variations in the surface height of typically several hundred nanometers, corresponding to the nanofiber diameters and pores in between. The necessary modifications of the control parameters to avoid the undesired adhesion of single nanofibers on the tip result in a lower resolution, as visible in Figure 4c in comparison with Figure 4b.

Taking MFM images is only possible in sample regions with moderate height variations, for example, on neighboring fibers with similar heights. Here, the maximum height differences were 130 nm (Figure 4c,g) and 35 nm (Figure 4d,h), respectively, where Figure 4d shows a small saturated part in the upper left area. The MFM images of the Co-coated films on the nanofiber mats show well-visible domain walls or out-of-plane stray fields, apparently along constrictions of the coated substrate, similar to other magnetic structures where constrictions reportedly worked as pinning sites [33–35]. Even in mostly even regions of the nanofiber mats, compromises had to be made between sufficient resolution of the magnetic features and proper control parameters. Figure 4g, for example, shows an apparently flat area in the upper left part of the image, corresponding to the maximum height, where the tip was too close to the surface for a correct MFM measurement.

CONCLUSION

To conclude, our experiments on Co-sputtered nanofiber mats, compared with sputtered wafer and polymer film substrates, show that MOKE measurements can unambiguously be performed on the highly refractive nanofiber mats, in this way receiving hysteresis loops similar to D-MOKE signals. It was shown that MFM measurements give rise to detecting magnetic domains or out-of-plane stray fields in Co-coated nanofiber mats. While MOKE and MFM measurements were previously reported on single nanofibers, our results for the first time demonstrate that measurements on randomly oriented nanofibers in electrospun nanofiber mats are also possible.

ACKNOWLEDGMENTS

The authors would like to thank Prof. G. Reiss for making available the ultrahigh vacuum sputtering system. Open Access funding enabled and organized by Projekt DEAL.

CONFLICT OF INTEREST STATEMENT

The authors declare no conflict of interest.

DATA AVAILABILITY STATEMENT

The data that support the findings of this study are available from the corresponding author upon reasonable request.

ORCID

Martin Wortmann http://orcid.org/0000-0002-5101-4643
Tomasz Blachowicz https://orcid.org/0000-0002-6569-124X
Andrea Ehrmann http://orcid.org/0000-0003-0695-3905

REFERENCES

[1] D.-H. Wang, J. Su, Y.-M. Liu, Y. Yu, Y. Su, G. X. Xie, L. L. Jiang, L. N. Zhou, D. Y. Zhu, S. H. Chen, J. S. Yan, X. X. Wang, Y. Z. Long, *J. Mater. Chem. C* **2022**, *10*, 4072.
[2] T. Blachowicz, A. Ehrmann, *J Eng Fibers Fabrics* **2020**, *15*, 155892501990084.
[3] K.-H. Na, W.-T. Kim, D.-C. Park, H.-G. Shin, S.-H. Lee, J. Park, T.-H. Song, W.-Y. Choi, *Thin Solid Films* **2018**, *660*, 358.
[4] X. Zuo, P. Xu, C. Zhang, M. Li, X. Jiang, X. Yue, *Ceram. Int.* **2019**, *45*, 4474.
[5] G. Bahrami, H. Ehzari, S. Mirzabeigy, B. Mohammadi, E. Arkan, *Mater. Sci. Eng. C* **2020**, *106*, 110183.
[6] C. Döpke, T. Grothe, P. Steblinski, M. Klöcker, L. Sabantina, D. Kosmalska, T. Blachowicz, A. Ehrmann, *Nanomaterials* **2019**, *9*, 92.
[7] L. Ourry, D. Le Roy, S. Mekkaoui, T. Douillard, A.-L. Deman, V. Salles, *Nanotechnology* **2020**, *31*, 395503.
[8] N. Fokin, T. Grothe, A. Mamun, M. Trabelsi, M. Klöcker, L. Sabantina, C. Döpke, T. Blachowicz, A. Hütten, A. Ehrmann, *Materials* **2020**, *13*, 1552.
[9] N. Ghazi, H. Mahmoudi Chenari, F. E. Ghodsi, *J. Magn. Magn. Mater.* **2018**, *468*, 132.
[10] E. Lage, R. Mattheis, J. McCord, *J. Magn. Magn. Mater.* **2019**, *487*, 165273.
[11] S. Torkian, A. Ghasemi, *J. Magn. Magn. Mater.* **2019**, *469*, 119.
[12] M. Jaafar, J. Pablo-Navarro, E. Berganza, P. Ares, C. Magén, A. Masseboeuf, C. Gatel, E. Snoeck, J. Gómez-Herrero, J. M. de Teresa, A. Asenjo, *Nanoscale* **2020**, *12*, 10090.
[13] A. Tillmanns, S. Oertker, B. Beschoten, G. Güntherodt, C. Leighton, I. K. Schuller, J. Nogués, *Appl. Phys. Lett.* **2006**, *89*, 202512.
[14] T. Blachowicz, A. Ehrmann, B. Mahltig, *AIP Adv.* **2017**, *7*, 045306.
[15] J. B. González-Díaz, J. A. Arregi, A. Martínez-de-Guerenu, F. Arizti, A. Berger, *J. Appl. Phys.* **2013**, *113*, 153904.
[16] S. Sahoo, A. May, A. van den Berg, A. K. Mondal, S. Ladak, A. Barman, *Nano. Lett.* **2021**, *21*, 4629.
[17] B. Myint, V. Ng, *Phys. Status Solidi Rapid Res. Lett.* **2021**, *15*, 2100197.
[18] M. Grimsditch, P. Vavassori, *J. Phys. Condens. Matter* **2004**, *16*, R275.
[19] J. Joshi, S. V. Homburg, A. Ehrmann, *Polymers* **2022**, *14*, 1267.
[20] M. Donolato, C. Tollan, J. M. Porro, A. Berger, P. Vavassori, *Adv. Mater.* **2013**, *25*, 623.
[21] K. Prashanthi, P. M. Shaibani, A. Sohrabi, T. S. Natarajan, T. Thundat, *Phys. Status Solidi Rapid Res. Lett.***2012**, *6*, 244.
[22] K. Prashanthi, T. Thundat, *Scanning* **2014**, *36*, 224.
[23] S. Choopani, F. Samavat, E. N. Kolobova, A. M. Grishin, *Ceram. Int.* **2020**, *46*, 2072.
[24] N. Liu, P. Du, P. Zhou, R. G. Tanguturi, Y. Qi, T. Zhang, *J. Am. Ceram. Soc.* **2021**, *104*, 948.
[25] R. Weiss, A. Ehrmann, *Commun. Dev. Assem. Text. Prod.* **2021**, *2*, 1.
[26] M. Trabelsi, A. Mamun, M. Klöcker, L. Sabantina, C. Großerhode, T. Blachowicz, A. Ehrmann, *Fibers* **2019**, *7*, 98.
[27] M. Li, Y.-P. Zhao, G.-C. Wang, H. G. Min, *J. Appl. Phys.* **1998**, *83*, 6287.
[28] T. Blachowicz, A. Ehrmann, *Coatings* **2021**, *11*, 122.
[29] K. S. Sivaranjani, G. Antilen Jacob, R. Justin Joseyphus, *J. Magn. Magn. Mater.* **2020**, *513*, 167228.
[30] T. Blachowicz, A. Ehrmann, *Spintronics—Theory, Modelling, Devices*, De Gruyter, Berlin/Boston **2019**.
[31] J. M. García, A. Thiaville, J. Miltat, *J. Magn. Magn. Mater.* **2002**, *249*, 163.
[32] M. Schwartzkopf, S. J. Wöhnert, V. Waclawek, N. Carstens, A. Rothkirch, J. Rubeck, M. Gensch, J. Drewes, O. Polonskyi, T. Strunskus, A. M. Hinz, S. J. Schaper, V. Körstgens, P. Müller-Buschbaum, F. Faupel, S. V. Roth, *Nanoscale Horiz.* **2021**, *6*(2), 132.
[33] M. Al Bahri, *J. Magn. Magn. Mater.* **2020**, *515*, 167293.
[34] H. Mohammed, S. A. Risi, T. L. Jin, J. Kosel, S. N. Piramanayagam, R. Sbiaa, *Appl. Phys. Lett.* **2020**, *116*, 032402.
[35] D. Kumar, T. Jin, R. Sbiaa, M. Kläui, S. Bedanta, S. Fukami, D. Ravelosona, S. H. Yang, X. Liu, S. N. Piramanayagam, *Phys. Rep.* **2022**, *958*, 1.

How to cite this article: O. Brocks, A. Stasiak, J. Biedinger, M. Wortmann, T. Blachowicz, R. Kaschuba, A. Ehrmann, *Appl. Res.* **2023**, e202200113.
https://doi.org/10.1002/appl.202200113